# A chromatic diversity index based on complex scenes

**João Manuel Maciel Linhares,[1,2,*] and Sérgio Miguel Cardoso Nascimento[2]**

[1]*Anglia Ruskin University, Faculty of Science and Technology, East Road, COS204, Cambridge CB1 1PT, UK*
[2]*Universidade do Minho, Centro de Física, Campus de Gualtar, Gualtar, 4710-057 Braga, Portugal*
**Corresponding author: joao.linhares@anglia.ac.uk*

Received September 1, 2011; revised November 22, 2011; accepted November 23, 2011;
posted November 28, 2011 (Doc. ID 153943); published January 26, 2012

We propose a chromatic diversity index based on the Munsell set capable of predicting illuminant induced changes in chromatic diversity of complex scenes. The color differences between complex scenes derived from hyperspectral data under a test and under a reference CIE D65 illuminant were computed and compared with the corresponding differences for the Munsell set. It was found that the average color difference between the complex scenes correlates well with the color differences of the Munsell samples with an average correlation of about 0.94, a result indicating that the Munsell set can be used to predict chromatic changes in complex scenes. 

*OCIS codes:* 330.1690, 330.1715, 330.1720, 330.6180.

## 1. INTRODUCTION

The spectral properties of the illumination determine the chromatic sensations experienced by observers in colorimetric tasks and everyday activities [1–3], as in illumination preferences for specific tasks [4] and chromatic discrimination [5], for example.

Some rendering properties of light sources are evaluated using only eight or fifteen standard colored samples as in the case of the color rendering index (CRI) [1] or the gamut area index (GAI) [6] and depend greatly on the resemblance of the light analyzed with daylight or black body radiator. Figure 1 represents the colored samples used in the computations of the CRI and of the GAI (the red dots in both cases). The use of a small number of chromatic samples may limit the use of such methods to describe color aspects of complex data. Other methods attempted to include chromatic discrimination as an additional parameter [6–12] but how well such methods describe color characteristics of more complex scenarios is still an open question. The use of the number of discernible colors [13–15] or the color volume enclosed by the optimal colors [16,17] have also been considered as a way of describing the chromatic diversity produced by different illuminants, but their computations are in general complex and very demanding in computational power. The use of the Munsell colored samples to describe the chromatic effects induced by different illuminants in complex scenarios of natural scenes can also be used to complement the CRI information [18].

The use of the LED and fluorescent light sources has been adopted increasingly due to energy efficiency. As these sources have spectra with marked spectral structure they present a new set of challenges to the evaluation of the light quality using the CRI. But can the full set of the Munsell samples (Fig. 1, gray open symbols) be a better chromatic database to estimate chromatic effects of complex illuminants and to predict its effects in complex scenes?

We addressed this question by comparing the colored effects produced by different illuminants on the CIELAB color volume of complex scenes derived from hyperspectral images and on the Munsell colored set. The goal was to investigate the use of a chromatic diversity index based on Munsell surfaces but capable of predicting the chromatic effects of more complex scenarios like natural scenes. Such an index is of high importance in applications were the chromatic diversity is chosen over color reproduction. The colors of 1269 Munsell surfaces and 85 hyperspectral images of natural, indoor, and artistic paintings scenes were simulated under 60 illuminants or light sources. Their CIELAB color volumes and the number of discernible colors were then computed and used as estimations of chromatic diversity. To understand better the chromatic effect on the CIELAB color volume, the color differences were also estimated.

## 2. METHODS

### A. Scene Database

Figure 2 represents thumbnails of some of the images of the database used. 85 scenes were used in the analysis: 50 images of natural scenes, 20 images of artistic paintings, 15 images of indoor scenes and spectral data of 1269 Munsell colored samples. The natural scenes, artistic paintings, and 12 indoor scenes represented in (a), (b) and (c) in Fig. 2, respectively, were imaged from 400 nm to 720 nm in 10 nm intervals using a fast-tunable liquid-crystal filter (Varispec, model VS-VIS2-10-HC-35-SQ, Cambridge Research & Instrumentation, Inc., Massachusetts) and a low-noise Peltier-cooled digital camera (Hamamatsu, model C4742-95-12ER, Hamamatsu Photonics K. K., Japan), capable of a spatial resolution of $1344 \times 1024$ pixels and 12 bit output (for more details on the hyperspectral system see Foster *et al.* [19]). The remaining three indoor scenes (represented as (d) in Fig. 2) are from Brainard's hyperspectral image database publicly available at (http://color.psych.upenn.edu/hyperspectral/index.html—last accessed 18-08-2011) acquired from 400 to 700 nm in 10 nm steps using narrowband interference filters and a monochromatic CCD camera with a spatial resolution of $2000 \times 2000$ pixels and 12 bit output [20].

 

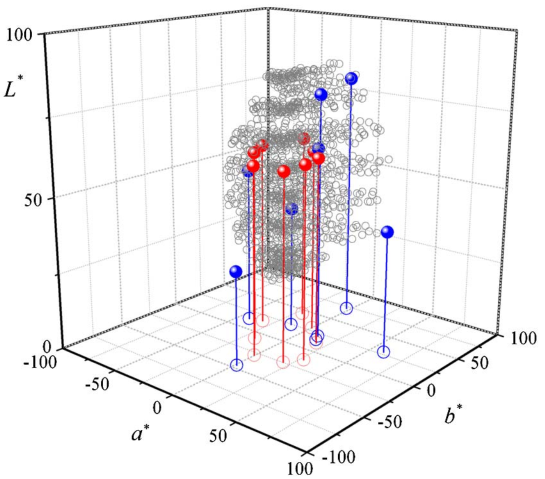


Fig. 1. (Color online) Representation on the CIELAB color space of the Munsell colored samples (open gray symbols) and the 15 CIE colored samples used in the estimation of the color rendering index (CRI) rendered under the CIE D65 illuminant (red symbols represent the eight colored samples used in the estimation of the general CRI and the blue symbols in combination with the eight red ones are used to estimate the special CRI).

In Brainard's hyperspectral images the spectral reflectance of each pixel was obtained by dividing the raw data by the illuminant spectrum of the scene obtained at a given reference location with a telespectroradimeter (SpectraColorimeter, PR-650, PhotoResearch Inc., Chatsworth, California).

For the natural scenes, artistic paintings, and indoor scenes obtained in our laboratory and represented as (a), (b), and (c), respectively, in Fig. 2, illuminant and optical spatial nonuniformities were minimized dividing the data obtained from the scene by the data obtained from a gray uniform reference imaged in the same place as the scene and under the same illuminant conditions [3,4]. The spectral reflectance of each pixel of the scene was estimated from a gray reference surface present in the imaged scene at the time of digitalization after corrections for dark noise, spatial nonuniformities, stray light, and chromatic aberrations.

The reflectance data from the Munsell surfaces was used as available at the spectral database, from the University of Joensuu Color Group, http://spectral.joensuu.fi/. Data was measured from 1269 colored samples from the Munsell Book of Color—Matte Finish Collection (Munsell Color, Baltimore, Maryland., 1976), from 380 nm to 800 nm in 1 nm steps, using a Perkin–Elmer lambda 9 UV/VIS/NIR spectrophotometer, as described in the details of the README file attached to the data.

The reflectance data was interpolated to 5 nm steps using a linear interpolation algorithm to adequate its spectral profile to the peak nature of some of the illuminants. The radiance data was estimated from the reflectance data by multiplying it by each illuminant spectrum from a set of 60 illuminants or light sources.

### B. Illuminant Database

Illuminants were considered from 400 nm to 720 nm for our and Munsell data and from 400 nm to 700 nm for Brainard's indoor data. The illuminants database was composed by tabulated CIE illuminants [21] and white LEDs light sources. Figure 3 represents the relative spectral power distribution of some of the CIE illuminants used that were: CIE illuminant A, C, 21 D illuminants including D55 and D65 (CCT in the range 25,000 K to 3,600 K in steps of 1190.3 K), 27 fluorescent illuminants (FL1, FL2, FL3, FL4, FL5, FL6, FL7, FL8, FL9, FL10, FL11, FL12, FL3.1, FL3.2, FL3.3, FL3.4, FL3.5, FL3.6, FL3.7, FL3.8, FL3.9, FL3.10, FL3.11, FL3.12, FL3.13, FL3.14, and FL3.15), and five high-pressure illuminants (HP1, HP2, HP3, HP4, and HP5).

Figure 4 represents the relative spectral power distribution of the white LEDs used: LXHL-BW02, LXHL-BW03, LXML-PWC1-0100, LXML-PWN1-0100, and LXML-PWW1-0060 from Luxeon, Philips Lumileds Lighting Company, USA. These LEDs were chosen because they are widely used and are commercialized by one of the main illumination companies.

The radiance data was then converted into tristimulus values for each illuminant assuming the CIE 1931 standard colorimetric observer [21] and then converted into color coordinates in the CIELAB color space. Figure 5 represents the effect of different illuminants on the CIELAB color volume of the colors of the image depicted. It was assumed that the image was rendered under the CIE D65 illuminant (image on the left) and under the CIE HP1 illuminant (image on the right).

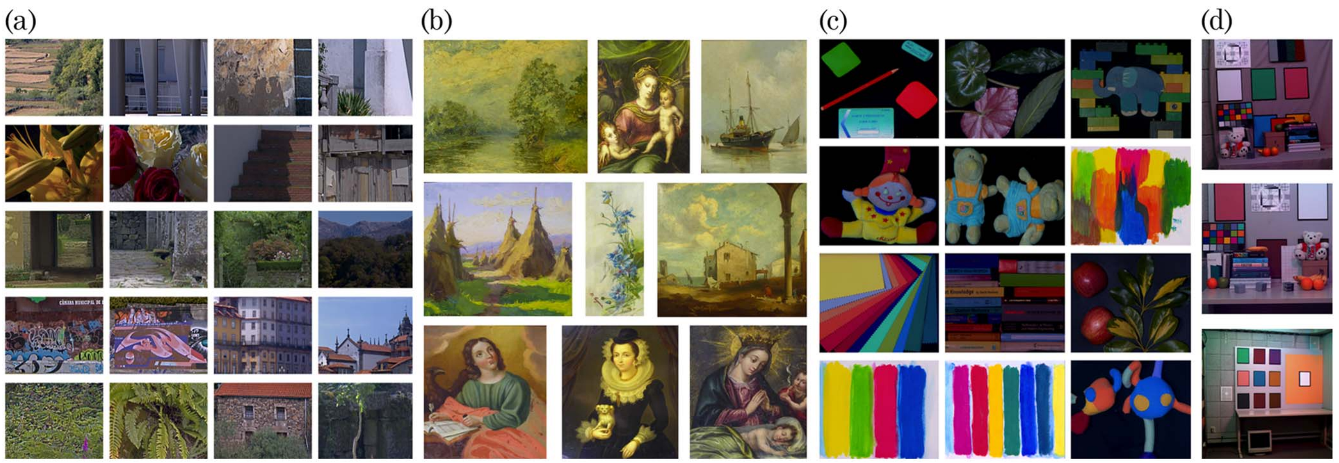


Fig. 2. (Color online) Thumbnails of some of the natural (a), art paintings (b), and indoor (c and d) images used in this work. The images represented in (d) are from David Brainard's hyperspectral image database, publicly available at (http://color.psych.upenn.edu/hyperspectral/index.html—last accessed 18-08-2011).

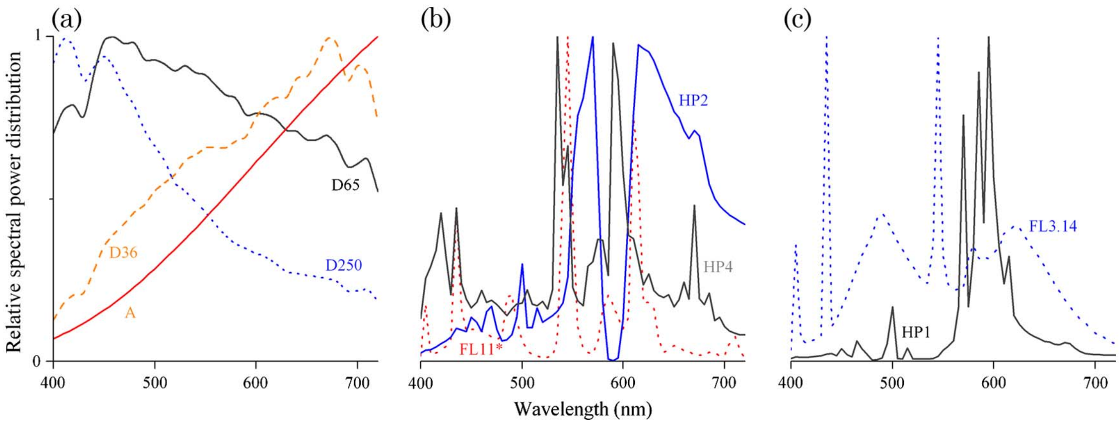


Fig. 3. (Color online) Normalized spectral power distribution of some of the CIE illuminants used in this work (adapted from [21]). (a) represents some daylight and CIE A illuminants and (b) and (c) represent some hi-pressure discharge and fluorescent CIE illuminants.

One coordinate in the drawn CIELAB color space represents a colored pixel from the represented image. Also shown and represented by the gray areas are the projections of the color volume in the individual $L^*$, $a^*$, and $b^*$ surfaces. It is evident the reduction on the chromatic content from the image rendered under the D65 illuminant when compared to the same image rendered under the HP1 illuminant.

Figure 6(a) represents a comparison of the area occupied by the chromaticity coordinates of the Munsell samples and the chromaticity coordinates of the hyperspectral data in the CIE $(a^*, b^*)$ color space assuming the projection of all $L^*$ levels ($L^* < 100$) in one level. All data was assumed rendered under the reference illuminant. Munsell samples occupy a smaller area (gray area) when compared to the data of the Brainard images (red dashed line), indoor images (blue dots line), natural images (green line), and art paintings (black line). The (b) panel represents examples of reflectance of Munsell colored samples and the (a) panel reflectance spectra from the hyperspectral data of the images analyzed. The data related to the natural images (green line) is consistent with former data obtained for CIE illuminant C [13].

### C. Estimation of the Color Differences

To understand better the chromatic effects of different illuminants in the Munsell set and its possible application in more complex scenes, the color differences in the CIELAB color space between the colors obtained using a test illuminant from the illuminants database and the ones obtained using the reference illuminant were computed and analyzed for all reflectance data. The CIE D65 illuminant was assumed as the reference illuminant in all the cases. Each reflectance spectrum was rendered under the test and reference illuminant and the color difference between the two colors was estimated.

To obtain detailed description across the color space, the analysis was performed in a segmented CIELAB color space for both complex scenes and Munsell colored samples. Figure 7 represents the segmentation of the CIELAB color space into 16 smaller subvolumes (figure on the left). The division into 16 subvolumes take into account the heavily computational resources needed to compute the data estimated here. Data was first divided from $L^* > 0$ to $L^* \leq 50$ (represented in orange) and from $L^* > 50$ to $L^* \leq 100$ (represented in blue). Each $L^*$ level was then divided into four quadrants: $a* > 0$ and $b^* > 0$, $a^* > 0$ and $b^* < 0$, $a^* < 0$ and $b^* < 0$, and $a^* < 0$ and $b^* > 0$. In each quadrant two separated volumes were assumed: one from 0 to 40 CIELAB units (represented in a continuous line) considered the inner volume and the other the remaining of the volume (represented in a dashed line) considered the outer volume in each quadrant. In the right panel of Fig. 7 it is represented the division in four quadrants of each $L^*$ level and its correspondent subdivisions, assuming only an $L^*$ level for simplicity. The segmentation was done assuming the reference illuminant. The average color

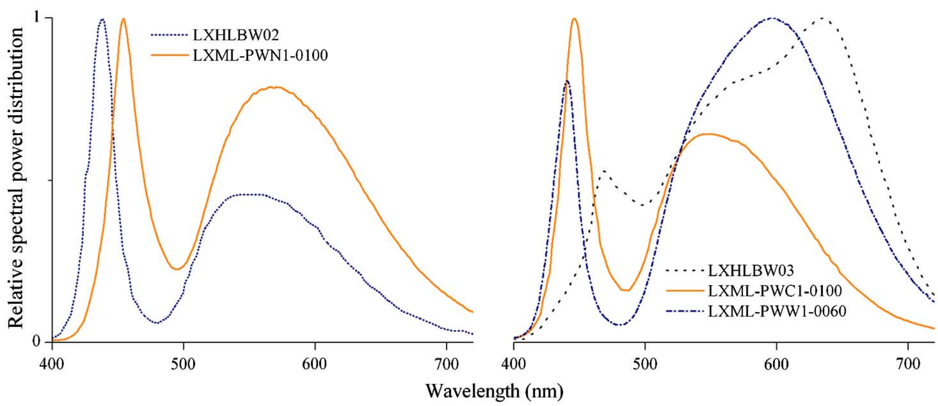


Fig. 4. (Color online) Normalized spectral power distribution of the LED light sources used in this work (from Luxeon, Philips Lumileds Lighting Company, EUA).

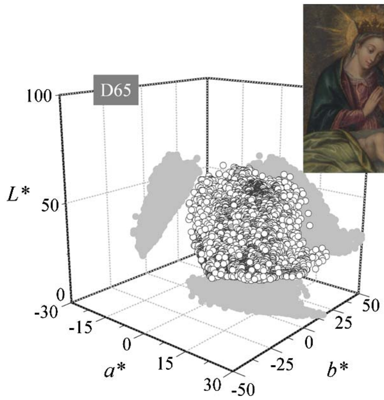


Fig. 5. (Color online) Influence of the spectral profile of an illuminant on the colors of an image of an art painting represented in the CIELAB color volume. Each point is a representation of a color from the art painting depicted rendered under the CIE D65 illuminant (on the left) and under the CIE HP1 illuminant (on the right). Gray areas represent projections of the color volume in the individual $L^*$, $a^*$, and $b^*$ surfaces.

difference was estimated in each subvolume and the data from the complex scenes was plotted as a function of the data from the Munsell scenes.

### D. Estimation of the Color Volumes and the Number of Discernible Colors

To use the chromatic effects produced by different illuminants on Munsell colored samples to describe the effects on more complex scenes, the volume occupied by the colors of the Munsell samples, and by the colors of the complex scenes was estimated in the CIELAB color space assuming the reflectance data rendered under the test and under the reference illuminant. To better characterize the chromatic effects of different illuminants on complex scenes, the number of discernible colors was also estimated for the hyperspectral images database, as no empty volumes are estimated with this technique when compared to the convex hull technique.

The volume occupied by the colors composing the CIELAB color volume for each complex scene, Munsell colored samples, and each illuminant was estimated using a convex hull algorithm (included in the software MATLAB 7.12.0.635 (R2011a), The MathWorks, Inc., Apple Hill Drive Natick, Massachusetts, USA) that computes the smallest convex polyhedron containing all of the points and estimates its volume.

The number of discernible colors was estimated by segmenting the CIELAB color volume into unitary cubes [13,14] and by counting the nonempty cubes. A unitary cube was assumed as a cube with one unit side and with a correspondent volume of 1 in the CIELAB color space. It was assumed that all the colors that were inside the same cube could not be discernible meaning that a filled cube represents a discernible color when compared to another filled cube.

The average of the color volume occupied by the colors of the complex scenes and corresponding number of discernible

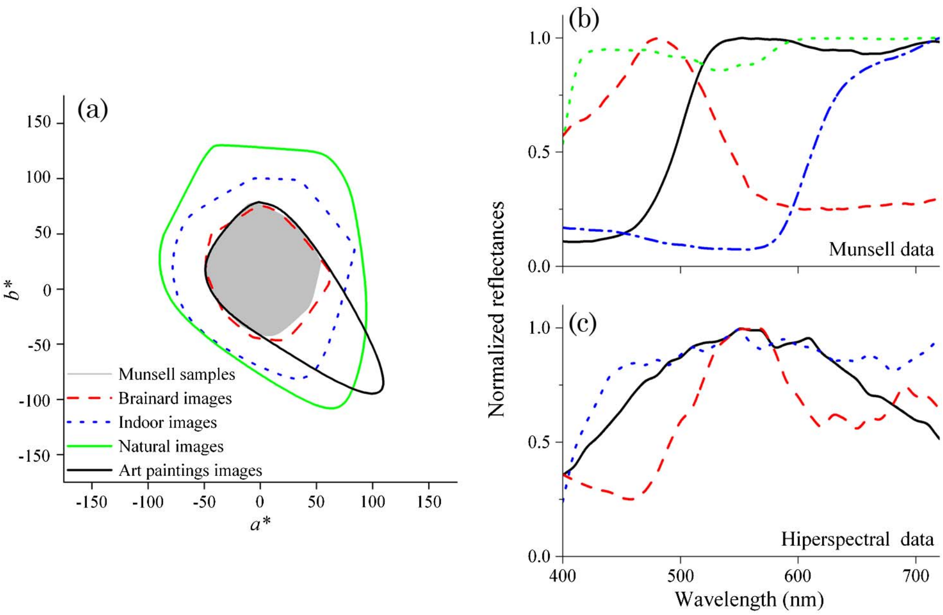


Fig. 6. (Color online) Left panel (a): area in CIE ($a^*$, $b^*$) color space occupied by the chromaticity coordinates of the Munsell samples (gray area) in comparison with the area occupied by the chromaticity coordinates of the data of the Brainard images (red dashed line), indoor images (blue dots line), natural images (green line), and art paintings (black line), assuming the projection of all $L^*$ levels ($L^* < 100$) in one level. All data was assumed rendered under the reference illuminant. Right panel: examples of reflectance data from Munsell colored samples (b) and the images of the scenes analyzed (c).

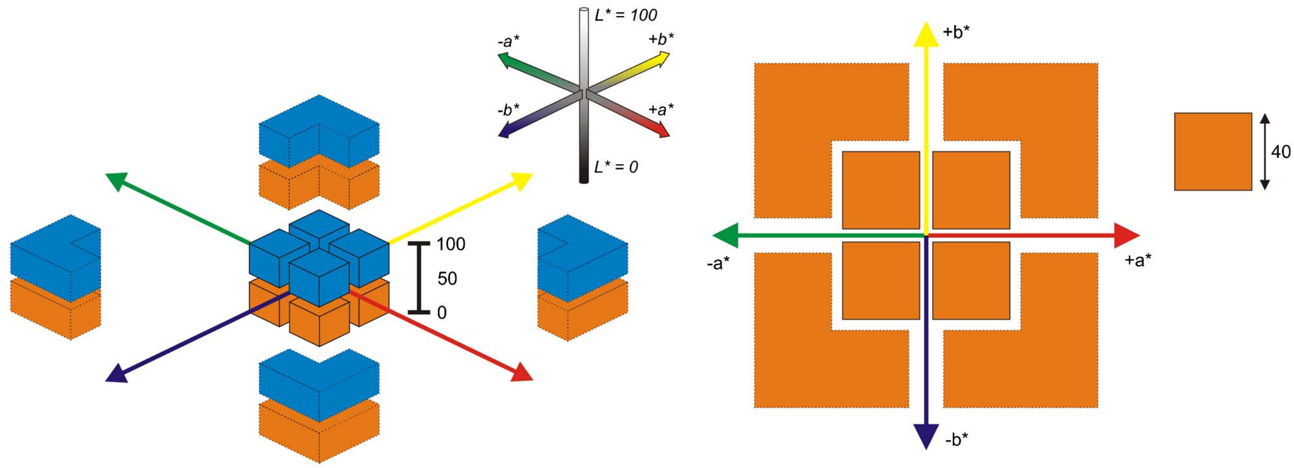


Fig. 7. (Color online) Division of the CIELAB color volume into 16 smaller subvolumes (figure on the left). Data was first divided from $L^* > 0$ to $L^* \leq 50$ (represented in orange) and from $L^* > 50$ to $L^* \leq 100$ (represented in blue). Each $L^*$ level was then divided into four quadrants: $a^* > 0$ and $b^* > 0$, $a^* > 0$ and $b^* < 0$, $a^* < 0$ and $b^* < 0$, and $a^* < 0$ and $b^* > 0$. In each quadrant two separated volumes were assumed: one from 0 to 40 CIELAB units (represented in a continuous line) and the other the remaining of the volume (represented in a dashed line). The right drawing represents such a division assuming for simplicity only an $L*$ level.

colors rendered under the test illuminant were estimated and then normalized to the color volume and number of discernible colors obtained with the reference illuminant, respectively. The color volume occupied by the Munsell colored samples rendered under the test illuminant was also estimated and normalized to the color volume obtained with the reference illuminant. The normalized color volumes and number of discernible colors of complex scenes were then plotted as a function of the volume occupied by the Munsell colored samples for illuminants tested.

## 3. RESULTS

Figure 8 represents the average across scenes of the average CIELAB color difference between the images rendered under the reference illuminant and the test illuminant or light source plotted as a function of the average CIELAB color difference of the Munsell colored samples rendered under the reference illuminant and the test illuminant. The data analysis was considered independently in each one of the subvolumes described in Fig. 7. The upper left image represents the $L^* > 50$ to $L^* \leq 100$ and the inner subvolumes in the four quadrants, the upper right image represents the $L^* > 50$ to $L^* \leq 100$ and the outer subvolumes in the four quadrants, the lower left image represents the $L^* > 0$ to $L* \leq 50$ and the inner subvolumes in the four quadrants, the lower right image represents the $L^* > 0$ to $L^* \leq 50$ and the outer subvolumes in the four quadrants. Straight lines represent unweighted linear regressions and the proportion of variance accounted for $R^2$ in the regression is also represented. No data is represented for the subvolume $L^* > 0$ to $L^* \leq 50$ with the outer subvolume of the quadrant corresponding to $a^* < -40$ and $b^* < -40$ because no Munsell data exist in that volume to compare. All the proportions of variance accounted for $R^2$ in the estimated regression were higher than 0.87, whenever data exist to perform the comparison.

Figure 9 represents in the top panel the average color volume of the complex scenes assumed rendered under the test illuminant, compared with the color volume obtained with the reference illuminant, plotted as a function of the color volume of the colors of the Munsell colored samples rendered under the test illuminant, compared with the color volume obtained with the reference illuminant. Data is presented for all the illuminants in the illuminants database. The lower panel in Fig. 9 represents the number of discernible colors perceived on the complex scenes. The data was assumed rendered under the test illuminant and compared with the number of discernible colors obtained with the reference illuminant, then plotted as a function of the color volume of the colors of the Munsell colored samples rendered under the test illuminant and compared with the color volume obtained with the reference illuminant. The same procedure was performed to all the illuminants in the illuminants database. Straight lines represent unweighted linear regressions and the proportion of variance accounted for $R^2$ in the regression and the correspondent adjusted linear equation are also represented. The proportion of variance accounted for $R^2$ in the linear regression when comparing the average of the volume occupied by the colors of the complex scenes and the volume of the colors of the Munsell colored samples is 0.85 with the linear equation of $y = 0.92x + 0.11$, while the one resulting from the comparison of the average of the number of discernible colors in complex scenes with the volume of the colors of the Munsell colored samples is 0.80 with the linear equation of $y = 0.73x + 0.3$. In Fig. 9 the point corresponding to the smaller color volume of the Munsell colored samples is relative to the CIE HP1 illuminant. The narrow profile of the spectral power distribution of CIE HP1 illuminant (as can be seen in Fig. 3) generates small amount of discernible colors or color volume. Since the data presented in Fig. 9 represents a ratio between the results obtained for each illuminant and the results obtained with the reference illuminant (CIE D65 illuminant), all data with a value higher than one represents an illuminant that performs better than D65. Examples of such illuminants are the CIE FL3.8 and FL 3.14 and several phases of daylight like the ones with correlated color temperature of 5208 K and 4490 K.

## 4. CHROMATIC DIVERSITY INDEX

The results presented here suggest that the Munsell colored samples can be used to estimate the chromatic diversity

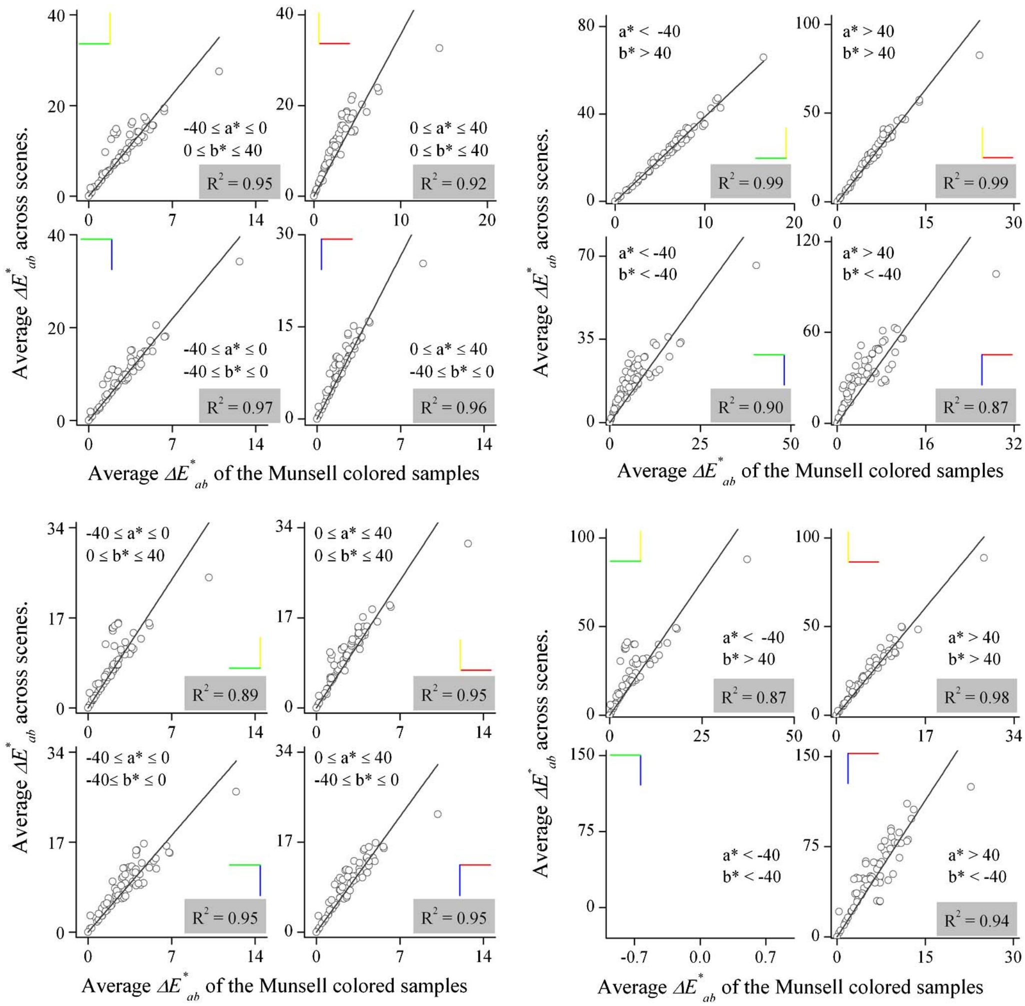


Fig. 8. (Color online) Average across scenes of the average CIELAB color difference between the images rendered under the reference illuminant and the test illuminant or light source plotted as a function of the average CIELAB color difference of the Munsell colored samples rendered under the reference illuminant and the test illuminant. The CIE D65 illuminant was assumed as the reference illuminant in each case. The data analysis was considered independently in each one of the subvolumes described in Fig. 7. The upper left image represents the $L^* > 50$ to $L^* \leq 100$ and the inner subvolumes in the four quadrants, the upper right image represents the $L^* > 50$ to $L^* \leq 100$ and the outer subvolumes in the four quadrants, the lower left image represents the $L^* > 0$ to $L^* \leq 50$ and the inner subvolumes in the four quadrants, the lower right image represents the $L^* > 0$ to $L^* \leq 50$ and the outer subvolumes in the four quadrants. Straight lines represent unweighted linear regressions and the proportion of variance accounted for $R^2$ in the regression is also represented. Colored lines are coded to represent the quadrants as represented in Fig. 7.

changes produced by several types of illuminants in complex scenes. The chromatic diversity index (CDI) results from the comparison of the volume occupied by the Munsell colored samples rendered under the test illuminant $V_{MT}$ divided by the volume occupied by the Munsell colored samples rendered under the reference illuminant $V_{MR}$, which could be the illuminant suggested by the CIE as the reference illuminant [21]. The volume occupied by the Munsell colored samples rendered under the CIE D65 illuminant is in absolute units 292740, estimated assuming the CIE 1931 standard colorimetric observer, the CIELAB color space, and the "*convhull*" function from the Matlab version 7.12.0.635 (R2011a) (The MathWorks, Inc., Apple Hill Drive Natick, Massachusetts USA). The CDI described in Eq. 1, assuming the CIE D65 illuminant as reference, is

$$\mathrm{CDI}_{D65} = V_{MT}/V_{MR} \times 100, \tag{1}$$

which can simply be

$$\mathrm{CDI}_{D65} = V_{MT}/2927.4. \tag{2}$$

Table 1 represents the general CRI, the volume occupied by the Munsell colored samples rendered under several CIE illuminants, and the correspondent CDI. Estimates considered the CIE 1931 standard colorimetric observer, the CIELAB color space, and the Matlab function "*convhull*" assuming the default function options.

The abscissa values of the top panel in Fig. 9 also represent the $\mathrm{CDI}_{D65}$, but in this particular case not as a percentage, since the volume of the Munsell colored samples are represented in relation to the volume occupied by the Munsell colored samples under the CIE D65 illuminant.

## 5. DISCUSSION

In this work we evaluated the use of the set of the Munsell colored samples as descriptors of the influence of several illuminants on the chromatic diversity of much more complex scenarios. Eighty-five hyperspectral images of natural, indoor,

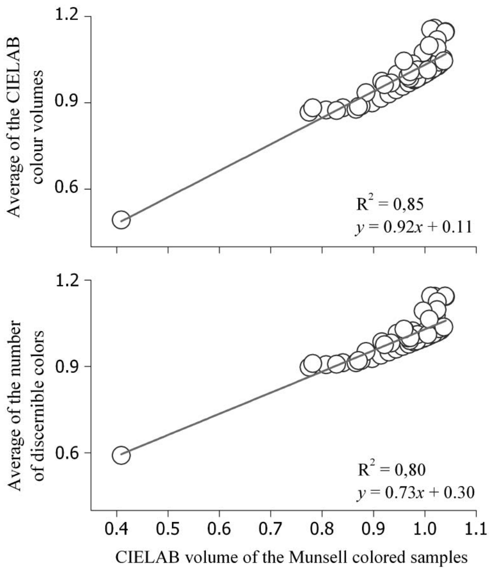


Fig. 9. Average of the color volume of the colors of the complex scenes (top panel) and its correspondent number of discernible colors (bottom panel) assumed rendered under the test illuminant and compared with the color volume and the number of discernible colors obtained with the reference illuminant, plotted as a function of the color volume of the colors of the Munsell colored samples rendered under the test illuminant and compared with the color volume obtained with the reference illuminant to all the illuminants in the illuminants database. Straight lines represent unweighted linear regressions and the proportion of variance accounted for $R^2$ in the regression and the correspondent adjusted linear equation are also represented.

and artistic paintings scenes were rendered with 60 CIE illuminants and LEDs light sources and the CIELAB color volume and the correspondent color differences accessed and compared with the same effect on the Munsell colored samples. CIE D65 illuminant was used as reference in all cases. It was found that the Munsell colored samples could reproduce the chromatic effects evaluated in 16 CIELAB subvolumes and on the number of discernible colors of much more complex scenes. These results support the introduction of a new index—the CDI—capable of predicting the effects of different illuminants on the chromatic diversity of complex scenes using the Munsell colored samples.

The existing correlation between the volume occupied by the Munsell colored samples and the average volume occupied by the complex scenes and the average number of discernible colors in such volumes is good, but not perfect. The illuminants that contribute greater to lower the degree of correlation are some fluorescent illuminants, probably due to the low signal in some areas of the visible spectrum and the very irregular spectral profile.

Several indices were proposed [6,12] to account the effect of the chromatic diversity produced by illuminants in complex scenes using reduced amount of chromatic information. Figure 10 represents the correlation between some of these indices with the color volume generated by a set of CIE illuminants on hyperspectral images of natural scenes. $R_{b1269}$ is the CRI estimated using 1269 different Munsell colored samples, $R_b$ is the special CRI, $R_a$ is the general CRI, GAI-8-UV is the GAI estimated using the eight colored samples used in the computation of the general CRI in the 1994 uniform color space [1], GAI-15-UV is the GAI estimated using the 15 colored samples used in the computation of the special CRI in the 1994 uniform color space, GAI-1269-UV is the GAI estimated using the 1269 Munsell colored samples in the 1994 uniform color space, Munsell is the volume occupied by 1269 the Munsell

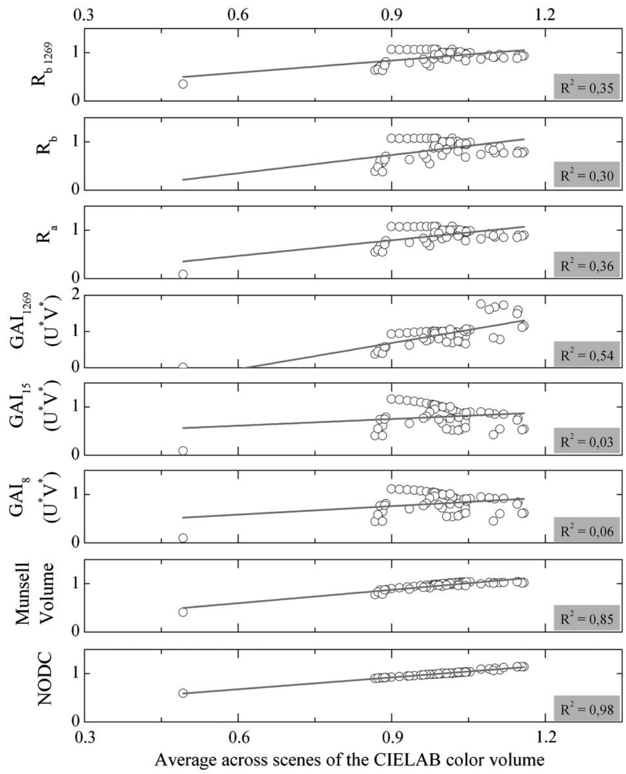


Fig. 10. Comparison of several methods of characterization of illuminants and light sources plotted as a function of the average volume occupied by the colors of complex scenes. $R_{b1269}$ is the CRI estimated using 1269 different Munsell colored samples, $R_b$ is the special CRI, $R_a$ is the general CRI, GAI-8-UV is the GAI estimated using the eight colored samples used in the computation of the general CRI in the 1994 uniform color space [1], GAI-15-UV is the GAI estimated using the 15 colored samples used in the computation of the special CRI in the 1994 uniform color space, GAI-1269-UV is the GAI estimated using the 1269 Munsell colored samples in the 1994 uniform color space, Munsell is the volume occupied by 1269 the Munsell colored samples in the CIELAB color space, NODC is the average number of discernible colors in complex scenes. Straight lines represent unweighted linear regressions and the proportion of variance accounted for $R^2$ in the regression is also represented.

**Table 1. General CRI and the Correspondent CDI Estimated for Several CIE Illuminants using Eq. (1), Assuming as Reference the CIE D65 Illuminant**

| Illuminant | CRI | $CDI_{D65}$ (%) |
|---|---|---|
| A | 100 | 98 |
| C | 80 | 98 |
| D50 | 100 | 102 |
| D75 | 100 | 98 |
| FL2* | 64 | 84 |
| FL7* | 90 | 97 |
| FL11* | 83 | 104 |
| FL3.14 | 95 | 104 |
| HP1 | 8 | 41 |
| HP4 | 74 | 95 |

colored samples in the CIELAB color space, NODC is the average number of discernible colors in complex scenes. Straight lines represent unweighted linear regressions, and the proportion of variance accounted for $R^2$ in the regression is also represented. The ones that better represent the average color volume of the complex scenes are the Munsell colored samples and the number of discernible colors [2,13,17].

The results presented here are based on computations using the CIELAB color space, known for its nonuniformities in particular in gray and blue areas [22,23]. The influence of these irregularities was also evaluated by estimating the color differences between the test illuminant and the CIE D65 illuminant in the DIN99d color space [24], again with no big influence in the final result. In the DIN99d color space the assumed color difference threshold was $DE = 0.6$ [17]. The segmentation of the color volume into discernible colors was done using unitary cubs and it was assumed that all the colors that are inside the same cube could not be distinguished, but in fact some colors inside the same cube have a color difference $\Delta E^*_{\mathrm{ab}} > 1$. The use of unitary spheres to segment the color volume can partially overcome this limitation, but some studies [13] suggest that relative estimates of the number of discernible colors are robust in relation to other methodologies that can be used to compute with great accuracy the number of discernible colors.

The CIELAB color space is also optimized to the CIE D65 illuminant [21] and the database of the illuminants used in this work has illuminants not comparable to the CIE D65 illuminant. To test the influence of the use of different illuminants in the CIELAB color space all the results were estimated including the effect of the CAT02 [25] chromatic adaptation. It was found that the influence of the chromatic adaptation was very small, without an impact in the final result [26].

Despite the limitations described here, the data presented in this work suggests that the Munsell colored samples can be used to estimate the effect of an illuminant in the chromatic diversity of complex scenes by the means of the CDI. The CDI can then be a good complement to the CRI and very useful in applications were the chromatic diversity is more important than their reproduction, like art galleries or indoor environments.

## ACKNOWLEDGMENTS

This work was supported by the Fundação para a Ciência e a Tecnologia (grant PTDC/EEA-EEL/098572/2008). We are grateful to Kinjiro Amano and David Foster for the use of the set of hyperspectral images. João Manuel Maciel Linhares partially supported by Ph.D. grant SFRH/BD/35874/2997 from the Fundação para a Ciência e a Tecnologia.

## REFERENCES

1. “Method of Measuring and Specifying Colour Rendering Properties of Light Sources,” CIE Publ. 13.3:1995 (CIE, 1995).
2. J. M. M. Linhares, P. E. R. Felgueiras, P. D. Pinto, and S. M. C. Nascimento, “Colour rendering of indoor lighting with CIE illuminants and white LEDs for normal and colour deficient observers,” Ophthalmic Physiol. Opt. **30**, 618–625 (2010).
3. J. M. M. Linhares, P. D. A. Pinto, and S. M. C. Nascimento, “Color rendering of art paintings under CIE illuminants for normal and color deficient observers,” J. Opt. Soc. Am. A **26**, 1668–1677 (2009).
4. P. D. Pinto, J. M. M. Linhares, and S. M. C. Nascimento, “Correlated color temperature preferred by observers for illumination of artistic paintings,” J. Opt. Soc. Am. A **25**, 623–630 (2008).
5. E. Mahler, J. J. Ezrati, and F. Vienot, “Testing LED lighting for colour discrimination and colour rendering,” Color Res. Appl. **34**, 8–17 (2009).
6. M. S. Rea and J. P. Freyssinier-Nova, “Color rendering: A tale of two metrics,” Color Res. Appl. **33**, 192–202 (2008).
7. W. A. Thornton, “Color-Discrimination Index,” J. Opt. Soc. Am. **62**, 191–& (1972).
8. W. A. Thornton, “Color-rendering capability of commercial lamps,” Appl. Opt. **11**, 1078–1086 (1972).
9. H. Xu, “Color-rendering capacity of illumination,” J. Opt. Soc. Am. **73**, 1709–1713 (1983).
10. W. Davis and Y. Ohno, “Color quality scale,” Opt. Eng. **49**, 33602–33616 (2010).
11. H. Xu, “Colour rendering capacity and luminous efficiency of a spectrum,” Lighting Res. Technol. **25** (1993).
12. C. Li and M. R. Luo, “Assessing colour rendering properties of daylight sources,” Ph.D. thesis (University of Leeds, (2008).
13. J. M. Linhares, P. D. Pinto, and S. M. Nascimento, “The number of discernible colors in natural scenes,” J. Opt. Soc. Am. A **25**, 2918–2924 (2008).
14. M. R. Pointer and G. G. Attridge, “The number of discernible colours,” Color Res. Appl. **23**, 52–54 (1998).
15. P. D. Pinto, P. E. R. Felgueiras, J. M. M. Linhares, and S. M. C. Nascimento, “Chromatic effects of metamers of D65 on art paintings,” Ophthalmic Physiol. Opt. **30**, 632–637 (2010).
16. E. Perales, F. Martínez-Verdú, V. Viqueira, M. J. Luque, and P. Capilla, “Computing the number of distinguishable colours under several illuminants and light sources,” in *CGIV 2006: Third European Conference on Color in Graphics, Imaging and Vision*, R. Luo, ed. (IS&T, 2006), pp. 414–419.
17. E. Perales, F. M. Martínez-Verdú, J. M. M. Linhares, and S. M. C. Nascimento, “Number of discernible colors for color-deficient observers estimated from the MacAdam limits,” J. Opt. Soc. of Am. A **27**, 2106–2014 (2010).
18. J. M. M. Linhares, P. D. A. Pinto, and S. M. C. Nascimento, “Chromatic Diversity Index—an approach based on natural scenes,” in CGIV 2010—5th European Conference on Colour in Graphics, Imaging, and Vision, and MCS’10, the 12th International Symposium on Multispectral Colour Science, J. Parkkinen and T. Jääskeläinen, eds. (2010), pp. 58–61.
19. D. H. Foster, K. Amano, S. M. C. Nascimento, and M. J. Foster, “Frequency of metamerism in natural scenes,” J. Opt. Soc. Am. A **23**, 2359–2372 (2006).
20. P. L. Vora, J. E. Farrell, J. D. Tietz, and D. H. Brainard, “Image capture: Simulation of sensor responses from hyperspectral images,” IEEE Trans. Image Process. **10**, 307–316 (2001).
21. “Colorimetry,” CIE Publ. 15:2004 (CIE, 2004).
22. M. R. Luo, G. Cui, and B. Rigg, “The development of the CIE 2000 colour-difference formula: CIEDE2000,” Color Res. Appl. **26**, 340–350 (2001).
23. M. D. Fairchild, *Color Appearance Models*, 2nd ed. (Wiley, 2005), p. 385.
24. G. Cui, M. R. Luo, B. Rigg, G. Roesler, and K. Witt, “Uniform colour spaces based on the DIN99 colour-difference formula,” Color Res. Appl. **27**, 282–290 (2002).
25. “A Review of Chromatic Adaptation Transforms,” CIE Publ 160:2004 (CIE, 2004), p. 30.
26. J. M. M. Linhares and S. M. C. Nascimento, “Color Diversity Index—the effect of chromatic adaptation,” in *International Conference on Applications of Optics and Photonics—AOP2011*, Manuel Filipe P. C. M. Costa, ed. [SPOF (Sociedade Portuguesa para a Investigação e Desenvolvimento em Óptica e Fotónica), 2011], paper 800104.